Dynamics of a Crash Victim—A Finite Segment Model

Ronald L. Huston,* Richard E. Hessel,†
and James M. Winget‡
University of Cincinnati, Cincinnati, Ohio

A vehicle-occupant, crash-simulation model is developed. The model consists of a finite-segment representation of the human body, together with a vehicle cockpit that includes a seat and crash intrusion surfaces (windshield, doors, etc.). The human body model is constrained to the cockpit by seat and shoulder belts. The equations of motion are developed for the model by using Lagrange's form of d'Alembert's principle. These equations then are coded into a computer program and solved numerically using a fourth-order Runge-Kutta method. Sample motions for several crash situations are presented and discussed.

Nomenclature

a^k = acceleration of G_k in R
B_k = bodies of the human model ($k = 2,\ldots, 12$)
F_k = external force applied to B_k
F_p = generalized active force
F_p^* = generalized inertia force
G_k = mass center of B_k
I_k = inertia dyadic of B_k relative to G_k
m_k = mass of B_k
M_k = external torque applied to B_k
O_k = reference point of B_k
r_k = mass center (G_k) position vector in B_k
R = inertial reference frame
v_{kji} = partial rate of change of position
x_i = generalized coordinates ($i = 1,\ldots,48$)
α^k = angular acceleration of B_k in R
ξ_k = reference point (O_k) position vector
ω^k = angular velocity of B_k in R

Introduction

During the past decade and especially during the past five years, there has been considerable research effort expended upon the development of finite-segment and finite-element models of structures and various dynamical systems. Of all of these models, perhaps the most extensive and imaginative effort has been in the development of finite-segment models of the human body and its dynamics, particularly in crash or high-acceleration environments. References 1-21 provide a summary of this research and its progress to date, with Ref. 1 providing a detailed comparison of the efforts. It suggests that the most elaborate models are those of Ref. 15 and 18. Success in these efforts has been related closely (although not exclusively) to advances in digital computer technology.

In this paper, the theoretical elements and basic features of a modern finite-segment, human-body, crash-victim model are presented. The paper is divided into five parts, with the first part describing the modeling process itself and the various associated theoretical problems. The second part presents the basic kinematics and dynamics of the model. The third part briefly discusses the specific features of the UCIN code, with some specific examples and illustrations presented in the fourth part. The final part of the paper presents some conclusions regarding the range of application of the model and some ideas regarding future model development.

Received March 28, 1975; presented as Paper 75-795 at the AIAA/ASME/SAE 16th Structures, Structural Dynamics, and Materials Conference, Denver, Colorado, May 27-29, 1975. The authors gratefully acknowledge support for this research by the Office of Naval Research under Contract N0014-72-A-0027-0002 and by the National Science Foundation under Grant GK-41272.

Index categories: Aircraft Cabin Environment and Life Support Systems; Computer Technology and Computer Simulation Techniques; Structural Dynamics Analysis.

*Department of Engineering Analysis. Associate Fellow AIAA.
†Department of Engineering Analysis.
‡Department of Engineering Analysis.

Finite-Segment Modeling

Finite-segment modeling in general, and more specifically human-body modeling, is perhaps most efficiently discussed in the context of modeling and of "general chain systems." A general chain system is defined to be a series of rigid bodies connected to each other in treelike fashion such that adjoining bodies share a common point and such that no closed loops are formed. Figure 1 shows an example of such a system.

The modeling and dynamics of general chain systems have been studied by Huston and Passerello,[22,23] Roberson,[24] Likins,[25-27] Chace and Bayazitoglu,[28] Hooker,[29] Fleischer,[30] and others. The basic difficulty encountered in all of these studies is the complexity of the geometry. This, in turn, presents difficulties in finding a kinematical description of the system and in obtaining the governing dynamical equation of motion. Huston and Passerello[22] have shown that the kinematics can be described conveniently and efficiently by using local coordinates (that is, angles between adjoining bodies) as opposed to absolute coordinates (that is, orientation angles in space) and by using a combined vector-matrix-tensor approach. They also maintain that using

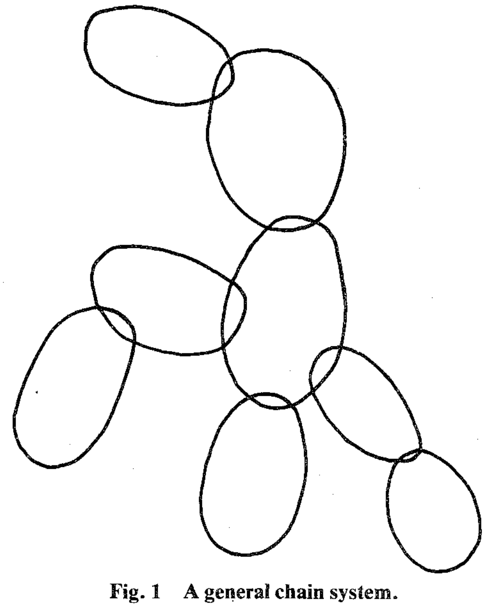

Fig. 1 A general chain system.

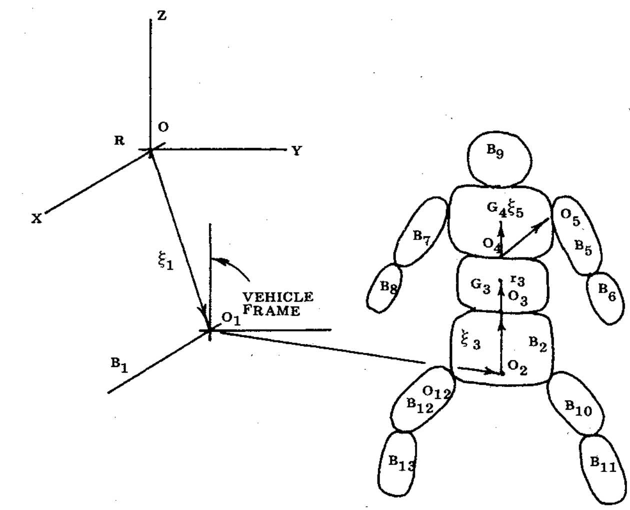

Fig. 2 The human-body model with a vehicle frame.

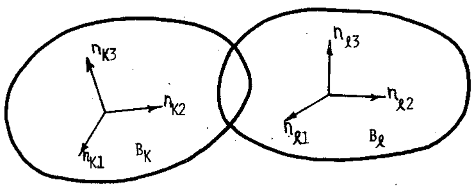

Fig. 3 Two typical adjoining bodies of the model.

Lagrange's form of d'Alembert's principle[31-34] is the most efficient way to obtain the governing dynamical equations of motion. They point out that Lagrange's form of d'Alembert's principle provides the exact number of governing equations (like Lagrange's equations, but not Newton's laws) and that it allows one to avoid lengthy involved differentiation of energy functions (like Newton's laws, but not Lagrange's equations). That is, for large complex systems, Lagrange's form of d'Alembert's principle incorporates the relative advantages of Lagrange's equations and Newton's laws while avoiding the corresponding disadvantages.

In this paper, the methods of Huston and Passerello are used to develop the governing equations of motion for a chain system representing a human-body model in a cockpit or vehicle frame as shown in Fig. 2. In this figure, the 12 rigid bodies are a spheriod, elliptical cylinders, and frustrumes of elliptical cones representing the various limbs of the human body. The system contains 42 degrees of freedom (6 for the translation and rotation of the vehicle frame, 6 for the translation and rotation of a reference body of the model relative to the vehicle frame, and 33 for the orientation of the 11 remaining bodies relative to their adjacent lower numbered bodies). The following section outlines the procedures used in obtaining the equations of motion for this system.

Kinematics and Equations of Motion

In Fig. 2, R represents an inertial reference frame, B represents the vehicle frame, and $B_2 \ldots, B_{13}$ represents the various limbs of the human-body model as shown. B_2 is the reference body of the model. O and O_1 are the origins (reference points) of R and B_1. O_2 is an arbitrarily chosen reference point of B_2. The reference points of each of the remaining bodies are the connecting points with the adjacent lower numbered bodies (e.g., O_3, O_4, $O_5, \ldots, O_{10}$). The vectors ξ_k $(k=1,\ldots,13)$ locate the reference points O_k $(k=1,\ldots,13)$ relative to the reference points of the adjacent lower numbered bodies. (Note that, except for ξ_1 and ξ_2, ξ_k is fixed in the adjacent lower numbered body.) The vectors r_k $(k=2,\ldots,13)$ locate the mass centers G_k *of* B_k relative to O_k.

Consider a typical pair of adjoining bodies of the model such as B_k and B_ℓ as shown in Fig. 3. Then the orientation of B_ℓ relative to B_k may be defined in terms of the relative inclination of the dextral, orthogonal unit vector sets $\boldsymbol{n}_{ki}$ and $\boldsymbol{n}_{\ell i}$ $(i=1,2,3)$, which are fixed, respectively, in B_k and B_ℓ. This is done as follows. Let B_k and B_ℓ be oriented so that $\boldsymbol{n}_{ki}$ and $\boldsymbol{n}_{\ell i}$ are respectively parallel. Then B_ℓ may be brought into any given orientation relative to B_k by three successive dextral rotations about axes parallel to $\boldsymbol{n}_{ki}$, $\boldsymbol{n}_{k2}$, and $\boldsymbol{n}_{k3}$ through the orientation angles $\alpha_{k\ell}$, $B_{k\ell}$, and $\gamma_{k\ell}$, $\boldsymbol{n}_{ki}$ and $\boldsymbol{n}_{\ell i}$ then are related to each other by the expressions§

$$\boldsymbol{n}_{ki} = SKL_{im} \boldsymbol{n}_{\ell m} \tag{1}$$

where SKL is a 3×3 orthogonal tranformation matrix defined as

$$SKL_{im} = \boldsymbol{n}_{ki} \cdot \boldsymbol{n}_{\ell m} \tag{2}$$

SKL may be written as the product of three orthogonal matrices as

$$SKL = \alpha KL \; \beta KL \; \gamma KL \tag{3}$$

where

$$\alpha KL = \begin{bmatrix} 1 & 0 & 0 \\ 0 & c\alpha_{k\ell} & -s\alpha_{k\ell} \\ 0 & s\alpha_{k\ell} & c\alpha_{k\ell} \end{bmatrix} \tag{4a}$$

$$\beta KL = \begin{bmatrix} c\beta_{k\ell} & 0 & s\beta_{k\ell} \\ 0 & 1 & 0 \\ -s\beta_{k\ell} & 0 & c\beta_{k\ell} \end{bmatrix} \tag{4b}$$

$$\gamma KL = \begin{bmatrix} c\gamma_{k\ell} & -s\gamma_{k\ell} & 0 \\ s\gamma_{k\ell} & c\gamma_{k\ell} & 0 \\ 0 & 0 & 1 \end{bmatrix} \tag{4c}$$

where $s\alpha_{k\ell}$ and $c\alpha_{k\ell}$ represent the sine and cosine of $\alpha_{k\ell}$. From Eq. (1), it easily is seen that, with three bodies B_k, B_ℓ, and B_m, the shifter transformation matrix obeys the following chain and identity rules:

$$SKM = SKL \; SLM \tag{5}$$

and

$$SKK = I = SKL \; SLK = SKL \; SKL^{-1} \tag{6}$$

These shifter matrices are used to transform the components of vectors and tensors referred to one body of the system into components referred to any other body of the system and, in particular, to the inertial frame R. It is necessary then also to have an expression for the derivative of the shifter matrix, especially the matrix SOK, where the O refers to the inertial frame R. Huston and Passerello[22,23] have shown that the derivative may be calculated by a simple matrix product as

$$S\dot{O}K = WOK \; SOK \tag{7}$$

where WOK is defined as

$$WOK_{im} = -e_{imn} \omega_n^k \tag{8}$$

§Regarding notation, repeated subscripts such as m in the right side of Eq. (1) represent a sum over the range $(1,\ldots,3)$ of that index.

where the e_{imn} is the standard permutation symbol[35] and ω_n^k are the components of the angular velocity of B_k referred to unit vectors n_{on} fixed in R.

The angular velocity ω^k of B_k in R is obtained from the addition formula[34]

$$\omega^k = \omega^I + {}^I\omega^2 + \ldots + {}^j\omega^k \tag{9}$$

where ${}^j\omega^k$ is the angular velocity of B_k relative to B_j. The series in Eq. (9) proceeds outward from B_1 to B_k through the branch of the chain or model containing B_k. From Fig. 2 and the preceding analysis, it easily is seen that ${}^j\omega^k$ may be expressed as

$$\begin{aligned}{}^j\omega^k = SOJ_{im}\,(\dot{\alpha}_{jk}\delta_{ml} + \beta_{jk}\alpha JK_{m2} \\ + \gamma_{jk}\alpha JK_{m\ell}\beta JK_{\ell 3})\,n_{oi}\end{aligned} \tag{10}$$

where δ_{mn} is Kronecker's delta symbol or identity tensor,[35] and $n_{oi}\,(i=1,2,3)$ are unit vectors fixed in R. By repeatedly substituting Eq. (10) into Eq. (9), ω^k can be seen to have the form

$$\omega^k = \omega_{kpm}\dot{x}_p n_{om} \tag{11}$$

where the $\dot{x}_p\,(p=1,\ldots,42)$ are the generalized coordinates representing the 42 degrees of freedom. By using Eq. (10), it is seen that the nonzero terms of ω_{kpm} take on of the following forms:

$$\omega_{kpm} = \begin{matrix} SOJ_{ml} \\ SOJ_{mn}\alpha JK_{n2} \\ SOJ_{mn}\alpha JK_{nh}\beta JK_{h3}\end{matrix} \tag{12}$$

depending upon whether x_p is the first, second, or third dextral angle (α, β, or γ) defining the orientation of B_k relative to its adjacent lower numbered body. Also, it is shown easily that, for any two bodies B_k and B_ℓ in the same branch of the model, $\omega_{\ell pm} = \omega_{kpm}$ for $\ell > k$ if $\omega_{kpm} \neq 0$.

The angular acceleration α^h of B_k in R may be obtained by differentiating in Eq. (11), that is,

$$\alpha^{lsk} = (\omega_{kpm}\ddot{x}_p + \dot{\omega}_{kpm}\dot{x}_p)\,n_{om} \tag{13}$$

where $\dot{\omega}_{kpm}$ may be obtained directly by differentiating in Eq. (12).

The velocity v^k of G_k, the mass center of B_k, relative to R may be obtained by differentiating the position vector p_k locating G_k relative to O. From Fig. 2, p_k is seen to have the form

$$p_i = \xi_I + \xi_2 + (\Sigma SOJ_{mn}\xi_n^j + SOK_{mn}r^k)\,n_{om} \tag{14}$$

where Σ indicates a sum over J (or j) for the bodies in the branch containing B_k $(j<k)$. Performing the differentiation in Eq. (14) shows that v^k may be written in a form analogous to Eq. (11) as

$$v^k = v_{kpm}\dot{x}_p n_{om} \tag{15}$$

where the v_{kpm} are obtained through using Eqs. (7) and (8).

The acceleration a^k of G^k in R may be obtained by differentiating in Eq. (15). That is,

$$a^k = (v_{kpm}\ddot{x}_p + \dot{v}_{kpm}\dot{x}_p)\,n_{om} \tag{16}$$

The governing dynamic equations of motion now may be obtained as follows. Consider again the model shown in Fig. 2. Let the externally applied forces be replaced by a system of forces consisting of single forces F_k passing through G_k $(k=1,2,\ldots,13)$ together with couples with torques M_k applied to B_k. Then Lagrange's form of d'Alembert's principle states that the governing equations of motion of the system are[34]

$$F_p + F_p{}^* = 0\;(p=1,\ldots,42) \tag{17}$$

where F_p is called the generalized active force and is given by

$$F_p = v_{kpm}F_{km} + \omega_{kpm}M_{km} \tag{18}$$

where F_{km} and M_{km} are the n_{om} components of F_k and M_k $(k=2,\ldots,13)$. $F_p{}^*$ is called the generalized inertia force and is given by

$$F_p{}^* = v_{kpm}F_{km}{}^* + \omega_{kpm}M_{km}{}^* \tag{19}$$

where $F_{km}{}^*$ and $M_{km}{}^*$ are n are n_{om} components of the inertia forces $F_k{}^*$ and inertia torques $M_k{}^*$, which, in turn, are[34]

$$F_k{}^* = -m_k a^k \qquad \text{(no sum)} \tag{20}$$

and

$$M_k{}^* = -I_k \cdot a^k - \omega^k x (I_k \cdot \omega^k) \qquad \text{(no sum)} \tag{21}$$

where m_k is the mass of B_k, and I_k is the inertia dyadic of B_k relative to G_k. Hence, by substituting from Eqs. (9-21), the equations of motion may be written in the form

$$a_{pq}\ddot{x}_q = f_p \quad (p,q=1,\ldots,42) \tag{22}$$

where a_{pq} and f_p are

$$a_{pq} = m_k v_{kpm} v_{kqm} + I_{kmn}\omega_{kpm}\omega_{kqn} \tag{23}$$

$$\begin{aligned} f_p = -\,(F_p + m_k v_{kpm}\dot{v}_{kqn}\dot{x}_q + I_{kmn}\omega_{kpm}\dot{\omega}_{kqn}\dot{x}_q \\ = e_{hmn}\omega_{kph}\omega_{kqm}\omega_{kri}I_{kni}\dot{x}_q\dot{x}_r)\end{aligned} \tag{24}$$

where I_{kmn} are the n_{om} components of I_k.

Equations (22) form a set of 42 simultaneous ordinary, nonlinear differential equations determining the 42 generalized coordinates x_p of the system. If some (or all) of the x_p are specified, then the differential equations become algebraic equations for the unknown forces or moments associated with the specified x_p. Since the coefficients a_{pq} and f_p of these equations are algebraic functions of the physical parameters and the generalized coordinates, the equations are ideally suited for generation on a digital computer.

UCIN Code

Algorithms have been written to develop the governing equations with a computer. These algorithms form the basic structure of the UCIN vehicle-occupant, crash-simulation code.[21] A number of special features then are added to simulate a vehicle-occupant system. These include 1) a vehicle (or cockpit) that can undergo up to six (three translation and three rotation) simultaneous accelerations; 2) an occupant seat rigidly attached to the vehicle frame consisting of up to seven springs and dampers of arbitrary moduli supporting the head, the upper middle and lower back, the tail, and the thighs; 3) up to 10 seat belts arbitrarily attached to the vehicle frame and the bodies of the human model; these belts are modeled as linear springs with arbitrary moduli; 4) arbitrary angle restraints at each joint of the human body model; these consist of dampers with arbitrary moduli; and 5) intrusion surfaces consisting of 13 planes of arbitrary position and orientation modeling the cockpit and providing a basis for "hits" of the human-body model with the cockpit. The governing equations then are solved numerically using a fourth-order, variable-step, Runge-Kutta integration routine. Input for the computer program consists of the physical data for the human-body model (masses and inertia matrices of the bodies, mass center position, and joining locations), the moduli for the various springs and dampers (see the foregoing), the number and attach points of the various seat belts, the cockpit intrusion surface geometry, and the vehicle

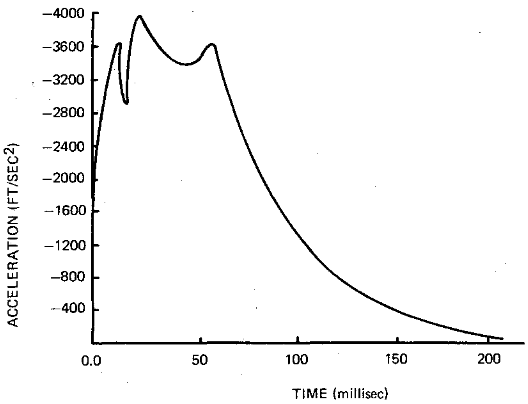

Fig. 4 Sled deceleration.

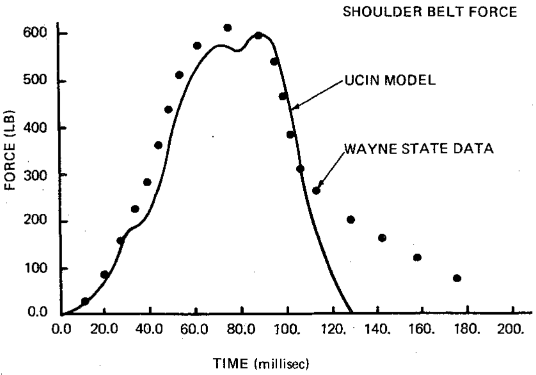

Fig. 5 Comparison of shoulder belt forces.

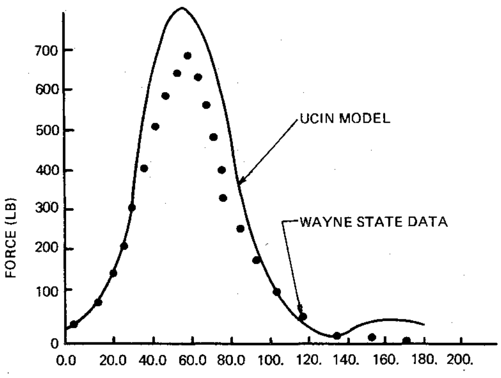

Fig. 6 Comparison of vertical lap belt forces.

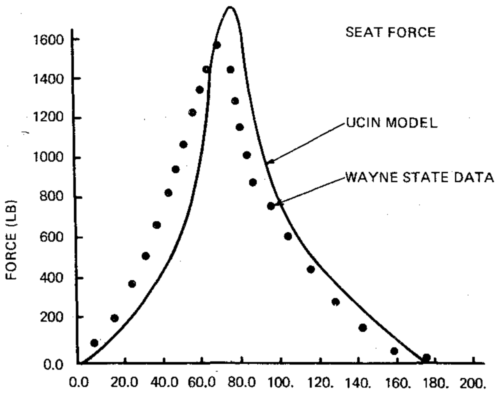

Fig. 7 Comparison of seat forces.

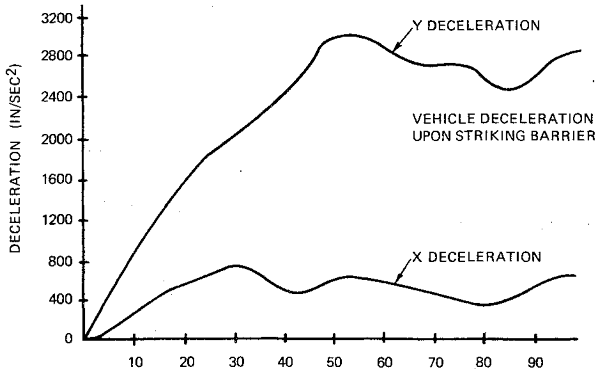

Fig. 8 Vehicle deceleration.

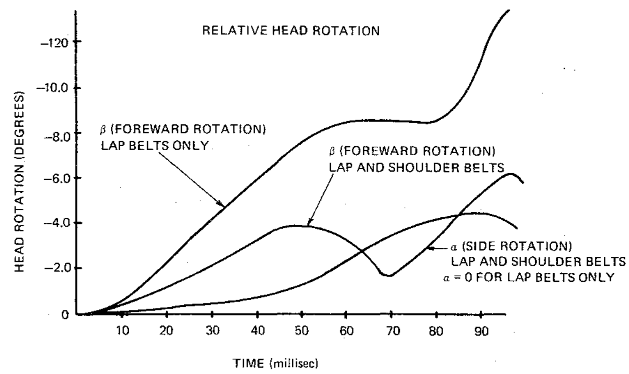

Fig. 9 Head rotation.

acceleration profile. The output consists of position, velocity, and acceleration profiles of the mass centers and joints relative to both the vehicle frame and inertia space.

The following section contains some illustrations of the use of the code. In each of these, the physical data input for the human-body model was taken from Hanavan[36] for his 50 percentile Air Force mean man. Either the other input data (springs and dampers) were selected to match those used in the experimental configuration, or moderate (i.e., average) values were assumed when no other source was available.

Verification and Examples

There is little experimental data available to date which can be used to check or verify the preceding computer code and others like it. However, an attempt at verification was made for some data gathered by King et al.[37] In these experiments, they placed a cadaver in a sled that impacted a stop, generating a sled deceleration profile, as shown in Fig. 4. The shoulder belt, vertical lap belt, and seat pan forces were measured. These forces then were calculated using the UCIN code with approximately the same sled (vehicle) deceleration profile and lap and shoulder belt configuration. (The acceleration profile was approximated by 25 straight line segments.) A comparison of the results is shown in Figs. 5-7.

In a second example, experimental data from a vehicle striking a guard rail or roadside barrier were used as input for the UCIN code. The specific acceleration profile and the resultant displacement of the head and chest using both lap belts and a combination of lap and shoulder belts is shown in Figs. 8-10.

Finally, in an attempt to measure the relative effectiveness of lap and shoulder belts, a run was made simulating a front-end collision of a vehicle. The head pitch of the model (forward rotation relative to the chest) was calculated using both lap belts and a combination of both lap and shoulder belts, as normally used in automobiles. The results, shown in Fig. 11,

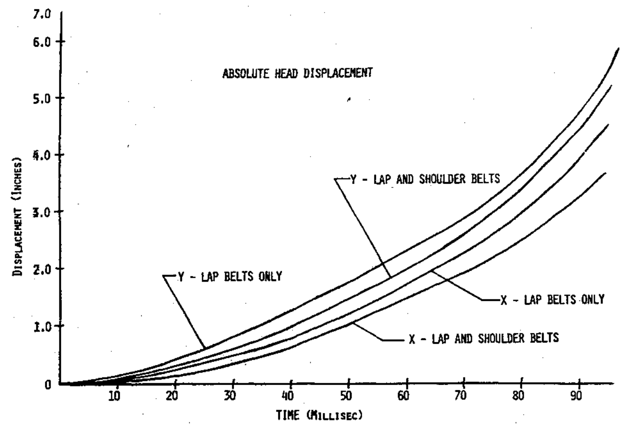

Fig. 10 Head displacement.

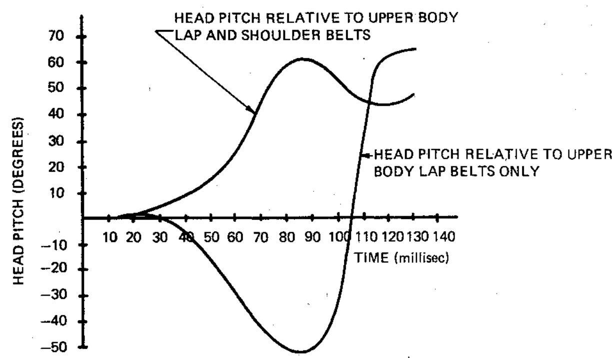

Fig. 11 Comparison of lap and shoulder belts.

clearly illustrate a "whiplash" effect when only lap belts are used.

Discussion and Conclusions

The analysis shows that it is now possible to construct reliable, finite-segment simulation models of crash vehicle occupants. The success of the modeling is due primarily to recent advances in digital computing machines and to new approaches in formulating the governing dynamical equations of motion.

The examples presented show the range of applicability of the model. In the particular cases studied, the advantages of combined shoulder and lap belt restraints as opposed to lap belts alone are remarkable, particularly in the prevention of "whiplash."

Finally, it appears that future work will include refinements of the model, particularly in vehicle (cockpit) and restraint modeling, model verification, and in making provision for variable numbers of human-body segments. Application of the model in the design of vehicle interior and safety devices is clear but is yet to be developed.

References

[1] King, A.I. and Chou, C.C., "Mathematical Modeling, Simulation and Experimental Testing of Biomechanical System Crash Response," Paper 75-272, Washington, D.C., 1975.

[2] McHenry, R.R., "Analysis of the Dynamics of Automobile Passenger Restraint Systems," *Proceedings of the 7th Stapp Car Crash Conference*, 1963, pp. 207-249.

[3] McKenzie, J.A. and Williams, J.F., "The Dynamic Behaviour of the Head and Cervical Spine during 'Whiplash,'" *Journal of Biomechanics,* Vol. 4, 1971, pp. 477-490.

[4] Segal, D.J. and McHenry, R.R., "Computer Simulation of Automobile Crash Victim-Revision," Rept. VJ-2492-v-1, 1967, Cornell Aeronautical Lab., Inc. Ithaca, N.Y.

[5] Segal, D.J., "Revised Computer Simulation of the Automobile Crash Victim," Rept. VJ-2759-v-2, 1971, Cornell Aeronautical Lab., Inc. Ithaca, N.Y.

[6] Danforth, J.P. and Randall, C.D., "Modified ROS Occupant Dynamics Simulation User Manual," Publ. GMR-1254, 1972, General Motors Corp. Research Labs, Detroit, Mich.

[7] Robbins, D.H., Bowman, B.M., and Bennett, R.O., "The MVMA Two-Dimensional Crash Victim Simulations," *Proceedings of the 18th Stapp Car Crash Conference*, 1974, pp. 657-678.

[8] Robbins, D.H., Bennett, R.O., and Roberts, V.L., "HSRI Two-Dimensional Crash Victim Simulator: Analysis, Verification, and Users' Manual," Final Rept. HSRI-Bio-M-70-8, 1970, University of Michigan, Highway Safety Research Institute, Ann Arbor, Mich.

[9] Glancy, J.J. and Larsen, S.E., "Users Guide for Program SIMULA," Rept TDR 72-23, 1972, Dynamic Science, Phoenix, Ariz.

[10] Robbins, D.H., "Three-Dimensional Simulation of Advanced Automotive Restraint Systems," *International Automotive Safety Conference Compendium,* Paper 700421, p-30, 1970, Society of Automotive Engineers.

[11] Robbins, D.H., Bennett, R.O., Jr., and Bowman, B.M., "User Oriented Matnematica Crash Victim Simulator," *Proceedings of the 16th Stapp Car Crash Conference*, 1972, pp. 128-148.

[12] Young, R.D., Ross, H.E., and Lammert, W.F., "Simulation of the Pedestrial During Vehicle Impact," *Proceedings of the 3rd International Congress on Automotive Safety,* Paper 27, Vol. ii, 1974.

[13] Furusho, H. and Yokoya, K., "Analysis of Occupant's Movement in Head-On Collision," *Transactions of the Society of Automotive Engineers of Japan*, No. 1, 1970, pp. 145-155.

[14] Bartz, J.A., "Development and Validation of a Computer Simulation of a Crash Victim in Three Dimensions," *Proceedings of the 16th Stapp Car Crash Conference, 1972, pp. 105-127.*

[15] Fleck, J.T., Butler, F.E., and Vogel, S.L., "An Improved Three Dimensional Computer Simulation of Motor Vehicle Crash Victims," Final TRZQ-5180-L-1, 1974, CALSPAN Corp. (in 4 vols), Ithaca, N.Y.

[16] Laananen, D., "Development of a Scientific Basis for Analysis of Aircraft Seating Systems," Rept. FAA-RD-74-130, Ultra Systems, Inc., Phoenix, Ariz.

[17] Huston, R.L. and Passerello, C.E., "On the Dynamics of a Human Body Model," *Journal of Biomechanics,* Vol. 4, 1971, pp. 369-378.

[18] Karnes, R.M. and Tocher, J.L. "Computer Simulation of a Vehicle Occupant in a Crash," Doc. BCS G0331, 1973, Boeing Computer Services, Inc., Seattle, Wash.

[19] Huston, R.L., Hessel, R.E., and Passerello, C.E., "A Three-Dimensional Vehicle-Man Model for Collision and High Acceleration Studies," Paper 740275, 1974, Society of Automotive Engineers Inc.

[20] Huston, R.L., Passarello, C.E., Harlow, M.W., and Winget, J.E., "The UCIN 3-D Aircraft-Occupant, Multisegment Model," *Symposium on Aircraft Crashworthiness,* Oct. 1975, Cincinnati, Ohio.

[21] Passerello, C.E., Huston, R.L., and Harlow, M.W., "User's Manual UCIN Vehicle-Occupant Crash Study Model—Version II," Rept. ONR-UC-EA—120174-3, 1974, University of Cincinnati.

[22] Huston, R.L. and Passerello, C.E., "On the Dynamics of Chain Systems," *ASME Winter Annual Meeting,* Paper 74-WA/Aut. 11, 1974, New York.

[23] Passerello, C.E. and Huston, R.L., "An Analysis of General Chain System," Rept. N72-30532, NASA-CR-127924, 1972.

[24] Roberson, R.E., "A Dynamical Formalism for an Arbitrary Number of Interconnected Rigid Bodies with Reference to the Problem of Satellite Attitude Control," *Proceedings of the 3rd International Congress of Automatic Control*, 1966, London, pp. 46D.1-46D.8.

[25] Likins, P.W., "Finite Element Appendage Equations for Hybrid Coordinate Dyanmic Analysis," *International Journal of Solids and Structures*, Vol. 8, 1972, pp. 709-731.

[26] Likins, P.W., "Dynamic Analysis of a System of Hinge Connected Rigid Bodies with Non Rigid Appendages," *International Journal of Solids and Structures*, Vol. 9, 1973, pp. 1473-1487.

[27] Likins, P.W., "Geometric Stiffness Characteristics of a Rotating Elastic Appendage," *International Journal of Solids and Structures,* Vol. 10, 1974, pp. 161-167.

[28] Chace, M.A. and Bayazitoglu, "Development and Application of a Generalized d'Alembert Force for Multifreedom Mechanical Systems," *Journal of Engineering for Industry,* 1971, pp. 317-327.

[29] Hooker, W.W., "A Set of r Dynamical Attitude Equations for an Arbitrary *n*-Body Satellite Having *r* Rotational Degrees of Freedom," *AIAA Journal*, Vol. 8, 1970, pp. 1205-1207.

[30]Fleischer, G.E., "Multi-Rigid Body Attitude Dynamics Simulator," TR32-1516, 1971, Jet Propulsion Laboratory.

[31]Huston, R.L. and Passerello, C.E., "On Lagrange's Form of d'Alembert's Principle," *The Matrix and Tensor Quarterly*, Vol. 23, 1973, pp. 109-112.

[32]Kane, T.R., "Dynamics of Nonholonomic Systems," *Journal of Applied Mechanics*, Vol. 28, 1961, pp. 574-578.

[33]Kane, T.R. and Wang, C.F., "On the Derivation of Equations of Motion," *Journal of the Society for Industrial and Applied Mathematics*, Vol. 13, 1965, pp. 487-492.

[34]Kane, T.R., *Dynamics*, Holt Rinehart, and Winston, N. Y., 1968.

[35]Brand, L. *Vector and Tensor Analysis*, Wiley N.Y. 1947.

[36]Hanavan, E.P., "A Mathematical Model of the Human Body," AMRL-TR-64-102, 1964, AMRL, Aerospace Medical Research Lab., Wright Patterson Air Force Base, Ohio.

[37]Begeman, P.C., King, A.I., and Prasad, P., "Spinal Loads Resulting from-G_x Acceleration," *Proceedings of the 17th Stapp Car Crash Conference*, 1973, pp. 343-360.

[38]Powell, G.H., "Computer Evaluation of Automobile Barrier Systems," Rept. FHWA-RD-73-73, 1970, Federal Highway Administration.